TABLE OF CONTENTS

SECTION PAGE

9. ATMOSPHERIC ELECTRICITY 9-1
9.1 Introduction 9-1
9.2 Cloud Electrification 9-1
9.2.1 Charge Separation Mechanisms 9-1
9.2.2 Thundercloud Electrical Structure 9-3
9.3 Frequency of Occurrence of Thunderstorms 9-3
9.3.1 Flash Counters 9-3
9.3.2 Lightning Location Systems 9-3
9.3.3 Satellite Observations 9-3
9.3.4 Thunder Day and Thunder Hour Statistics 9-6
9.3.5 Thunderstorm Characteristics 9-6
9.4 Cloud-to-Ground Lightning Damage and Protection 9-6
9.4.1 Characteristics of Cloud-to-Ground Discharges 9-9
9.4.2 Lightning Current Damage Parameters 9-10
9.4.3 Tower Measurements of Current 9-10
9.4.4 Triggered Lightning Current Measurements 9-14
9.4.5 Inferring Damage Parameters From Lightning Fields 9-14
9.5 Lightning Test Standards 9-19
9.5.1 Historical Perspective 9-19
9.5.2 Severe Direct Lightning Strike Current Test Waveforms 9-20
References 9-27

This Page Left Blank Intentionally

SECTION 9

ATMOSPHERIC ELECTRICITY

9.1 Introduction. Atmospheric electricity must be considered in the design, transportation, and operation of aerospace vehicles. Aerospace vehicles that are not adequately protected can be upset, damaged, or destroyed by a direct lightning stroke to the vehicle or the launch support equipment while on the ground or after launch (e.g., Refs. 9.1, 9.2, and 9.3). Damage can also result from the current induced in the vehicle from changing electric fields produced by a nearby lightning stroke. The effect of the atmosphere as an insulator and conductor of high-voltage electricity at various atmospheric pressures must also be considered. High voltage systems aboard the vehicle which are not properly designed can arc or breakdown at low atmospheric pressure.

This section provides an introductory description of the electrification of thunderclouds and thundercloud electrical structure (Section 9.2) and gives the reader a basic understanding of the frequency of occurrence of thunderstorms across the United States (Section 9.3). The characteristics of cloud-to-ground lightning discharges are then discussed in detail in Section 9.4 with emphasis on lightning damage and protection. In Section 9.4, four lightning current damage parameters that are important in determining protective measures against lightning are described, and estimates of these parameters from tower strike measurements, rocket triggered lightning experiments, and field inferred methods are given. A NASA TM – pending publication (Ref. 9.47) entitled *"NASA Kennedy Space Center Peak Lightning Current Probabilities: Analysis and Assessment,"* addresses the estimation of the probabilities of various high current lightning strikes to the Shuttle during its rollout through ascent.

Finally, Section 9.5 is devoted to lightning current test standards that have recently been adopted for improving the protection of aerospace vehicles (Refs. 9.4 and 9.5). Severe lightning strike current test waveforms are provided that are more realistic than the test waveforms provided in the prior revision of this document (NASA TM 82473). In this section, five current test waveforms are given which can be used in the design, development, and test of aerospace vehicles. These test waveforms represent components of a severe lightning strike event.

9.2 Cloud Electrification. Under the proper meteorological conditions, a moist region of the atmosphere may be lifted by a variety of external forcings (e.g., surface heating, terrain effects, fronts, etc.). In very unstable atmospheres, this lifting may result in the development of a cumulonimbus cloud (or thundercloud) whose cloud top extends to altitudes where the ambient air temperature is well below freezing. The electrified nature of a thundercloud is fundamentally related to processes occurring at both the microphysical and cloud-size scales.

9.2.1 Charge Separation Mechanisms. There have been important recent developments in understanding the processes responsible for the electrification of thunderstorms due to increasingly realistic laboratory simulations, and cooperative experiments combining simultaneous observations of electrical and microphysical parameters and the use of sophisticated methods of following air motions.

Table 9.1 summarizes a variety of charge separation processes that occur at the microphysical and cloud-size scales (Ref. 9.6). These processes vary in importance depending on the developmental stage of convective clouds. However, it has been suggested that both induction and interface charging are the primary electrification mechanisms in convective clouds (Ref. 9.7). Inductive charging involves bouncing collisions between particles in the external field. The amount of charge transferred between the polarized drops at the moment of collision depends on the time of contact, the contact angle (no charge transferred at grazing collisions), the charge relaxation time, and the net charge on the particles. Interface charging involves the transfer of charge due to contact or freezing potentials during the collisions between riming

precipitation particles and ice crystals. The sign and magnitude of the charge transfer depended on the temperature, liquid water content, and the ice crystal size and impact velocity.

Table 9.1 Charging mechanisms in clouds and thunderstorms (ref. 9.8).

Mechanism	Microscale	Cloud Scale	Major Roles
1. Diffusion charging	Ion capture by diffusion		Removes ions within cloud
2. Drift charging	Ion capture in drift currents	Drift currents Convection (Sedimentation)	Charges particles Enhances field
3. Selective ion charging	Ion capture by polarized drops	Sedimentation (Convection)	Charges particles Enhances fields
4. Breakup charging	Collisional breakup of polarized drops	Sedimentation (Convection)	Charges drops
5. Induction charging	Charge transfer between polarized particles	Sedimentation (Convection)	Charges particles Enhances field
6. Convection charging	Space-charge production Ion capture in drift currents	Convection	Enhances field (Charges particles)
7. Thermoelectric charging	Charge transfer between particles of differing temperatures	Sedimentation (Convection)	(Charges particles)
8. Interface charging	Charge transfer between particles involving contact potentials (freezing potentials)	Sedimentation (Convection)	Charges particles Enhances field

9.2.2 Thundercloud Electrical Structure. Figure 9.1 illustrates the vertical charge structure of a thundercloud for different geographical locations. A tripolar charge structure is often evident, with a spatially extended region of positive charge at high altitudes, a narrow band of negative charge at lower altitudes, and a small pocket of positive charge near cloud base (Ref. 9.8). The thundercloud charge distribution has been inferred using a variety of in situ (e.g., balloon, aircraft) and remote measurements. For instance, ground-based measurements of lightning field changes obtained from a field mill network at the Kennedy Space Center (KSC) have been analyzed to determine the charges deposited by lightning in Florida thunderstorms (Ref. 9.9). Figure 9.2 summarizes some of these results. The circles represent negative charge centers associated with cloud-to-ground lightning, while the vectors indicate moment charges due to cloud discharges. These results are consistent with the charge distribution given in Figure 9.1.

9.3 Frequency of Occurrence of Thunderstorms. An important phenomenological parameter that aids in the design of lightning protection systems is the average lightning flash density, i.e., the number of lightning ground strikes per square kilometer per year. This parameter is critical in almost all lightning protection designs (such as the lightning overvoltage protection of a utility power line), since the number of power outages or related failures are directly proportional to the number of cloud-to-ground discharges per unit area per year (Ref. 9.10). Various ways of obtaining flash densities are given below along with some results.

9.3.1 Flash Counters. Most available data on lightning flash densities have been derived from flash counters. Reference 9.11 has summarized much of the published and unpublished data on average flash density that have been obtained using flash counts, visual observations, and electric field change meters. The mean annual flash density for the United States is given in Figure 9.3.

9.3.2 Lightning Location Systems. The development of techniques during the last decade for the automatic detection and location of cloud-to-ground lightning strike points represents an important recent advance in lightning and thunderstorm observations. Systems based on magnetic direction finding (Ref. 9.12) and on time-of-arrival techniques have been developed and deployed in networks that cover large regions worldwide, including the continental United States and Alaska. With these systems, thunderstorms can conveniently be monitored and tracked from the cloud-to-ground lightning that they produce. Climatic statistics on ground strike flash densities derived from these lightning location systems are now becoming available.

9.3.3 Satellite Observations. Satellites represent ideal platforms for observing lightning over large regions of the Earth. Already, instruments carried on satellites in low-Earth orbit have provided additional data on the geographical and seasonal distribution of thunderstorms and lightning. New information has been gathered, in particular, for regions over the oceans which could not be monitored using flash counters or lightning location systems. These measurements have suffered from low detection efficiency, poor spatial resolution, and the inability to continuously monitor specific storms or storm systems.

Using results of recent thunderstorm investigations that include observations with high altitude NASA U-2 aircraft, space sensors capable of mapping both intracloud and cloud-to-ground lightning discharges during the day and night with a spatial resolution of 10 km (i.e., storm scale resolution) and high detection efficiency (i.e., 90 percent) are planned for the late 1990's. One such instrument, the lightning mapper sensor (LMS), is planned for placement in geostationary Earth orbit on a geostationary operational environmental satellite (GOES) (Ref. 9.13). Another instrument called the lightning imaging sensor (LIS) has been selected for the Tropical Rainfall Measuring Mission (TRMM) and a lightning detector system with significantly improved capabilities can be expected for the geostationary platform. The LMS, LIS, and other satellite-based lightning detection systems will support Earth system science studies in the next decade and beyond.

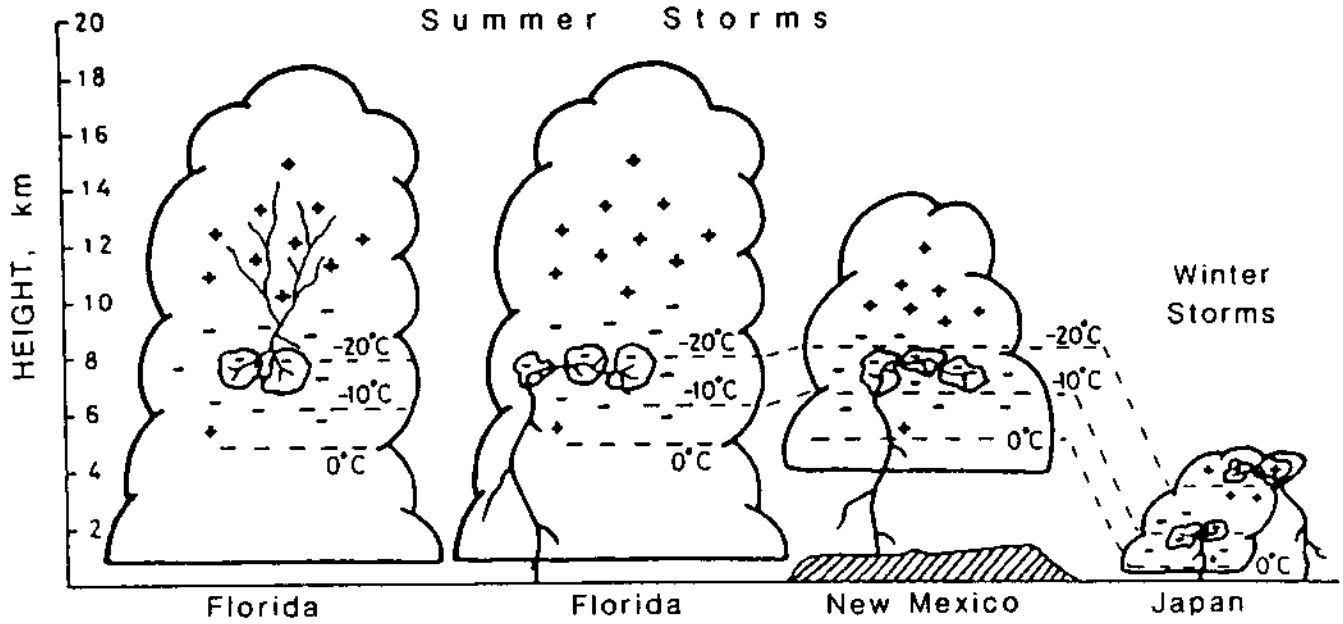

FIGURE 9.1 Negative Charge Centers at Similar Temperature Levels for Storms in Different Locations (Ref. 9.8).

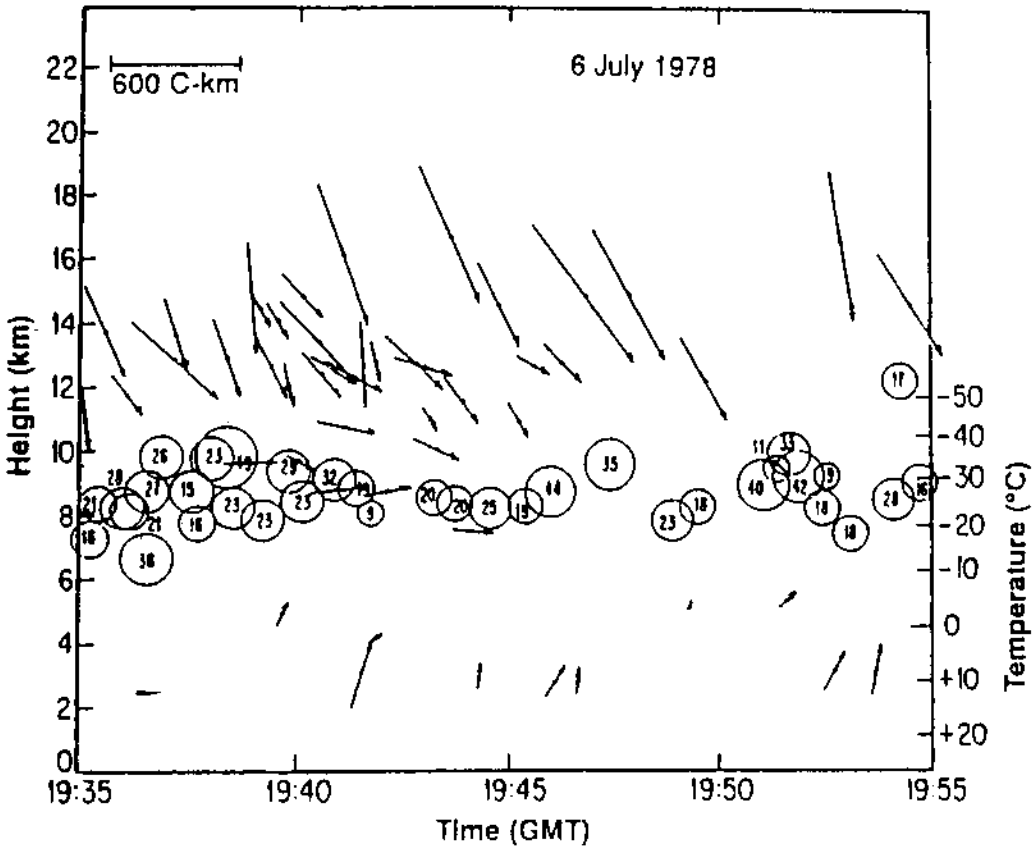

FIGURE 9.2 Charges Deposited by Lightning in a Florida Thunderstorm (Ref. 9.9).

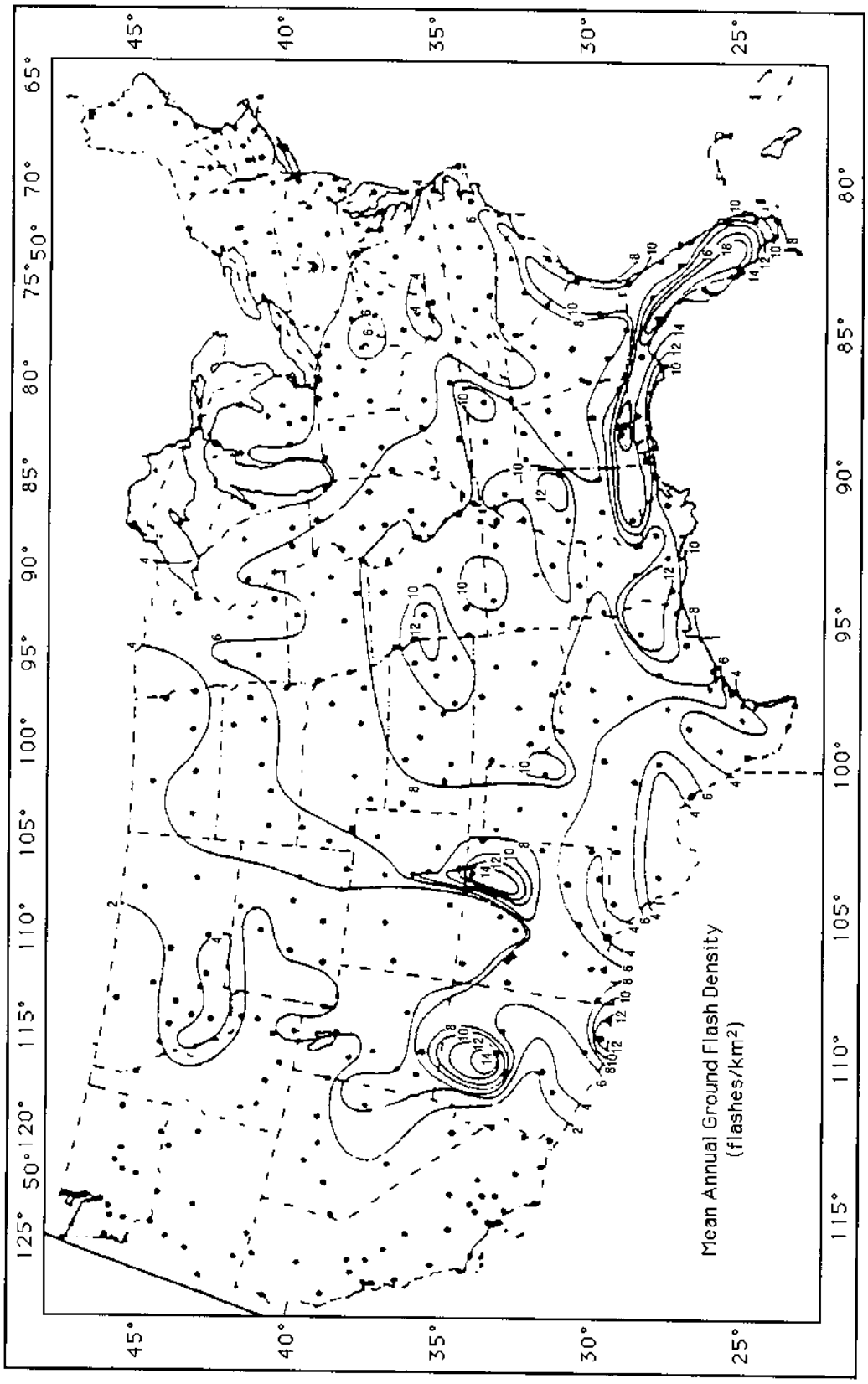

Figure 9.3 Mean annual U.S. ground strike density (ref. 9.14).

9.3.4 Thunder Day and Thunder Hour Statistics. Audible thunder is an indication of nearby thunderstorm activity, and its occurrence is recorded routinely at meteorological stations around the world. If thunder is heard one or more times in a day, that day is counted as one "thunder day." These data provide the most readily available and longest-term measurement of world-wide thunderstorm occurrence. A compilation of world-wide thunder day data has been given by the World Meteorological Organization (Ref. 9.14) and the isoceraunic level, or number of thunder days per year, is plotted in Reference 9.15. Thunder day data from 227 global stations have recently been examined for secular variations during the period 1901 to 1980 (Ref. 9.16).

Thunder day statistics for the 33-year period from 1957 to 1989 at KSC are given in Tables 9.2 and 9.3 as a function of year, month, and time of day. Figure 9.4 presents the incidence of thunderstorm days (days thunderstorms observed) annually for the United States (Ref. 9.17a). Monthly U.S. thunderstorm frequencies can be obtained from Reference 9.17b.

For many applications, however, thunder day statistics are inadequate because (1) the duration of lightning activity is unknown, (2) the data do not provide a measure of lightning flashing rates, (3) there is no distinction made between intracloud and cloud-to-ground discharges, and (4) the range of audibility of thunder may be quite variable and depends on station location and atmospheric conditions.

A somewhat more precise measurement of thunderstorm activity is by thunderstorm duration (measured in thunder hours). It is defined as the difference between the time thunder was first heard and a time 15 minutes after the last occurrence of thunder. Since it is the ground flash density (N_g) that is important in lightning protection design, empirical relations have been found to relate thunder days (T_D) and thunder hours (T_H) to N_g. These relations are of the form:

$$N_g = a(T_D)^b$$
$$N_g = c(T_H)^d \quad , \tag{9.1}$$

where the values of the constants *a, b, c,* and *d* vary from study to study as indicated in reference 9.10.

9.3.5 Thunderstorm Characteristics. The frequency of thunderstorm durations across the U.S. can be obtained from 9.18, whereas the diurnal variation of U.S. thunderstorms is available from 9.19. A specific climatological study of Florida summer thunderstorms is documented in 9.20. A severe thunderstorm climatology presenting extreme hail-fall and the associated strong winds is given in 9.21. The extreme hail characteristics given in 9.21 are also presented in Section 7.5 of this document.

9.4 Cloud-to-Ground Lightning Damage and Protection. Damaging effects due to lightning include human injury or death, forest fires, communication and power system failures, and hazards to civil, commercial, and military aircraft and aerospace vehicles. In order to determine valid protection standards, it is necessary to investigate the basic characteristics of a lightning discharge. Knowledge of lightning currents and radiation fields is fundamental in this understanding, and recent data on these quantities are discussed below. This section will concentrate primarily on ground discharges.

TABLE 9.2 Number of Thunderstorm Days at KSC by Month, for Each Year.

	MONTHS												
YEAR	1	2	3	4	5	6	7	8	9	10	11	12	YR SUM
1957	0	0	3	1	12	9	16	15	10	2	1	2	71
1958	1	2	4	3	5	10	8	14	9	2	1	0	59
1959	1	1	2	5	9	11	10	10	11	5	0	0	65
1960	0	2	4	3	6	17	21	11	9	4	0	0	77
1961	0	0	4	3	6	13	8	14	7	2	0	1	58
1962	0	3	3	3	4	17	19	22	10	3	1	0	85
1963	1	1	2	2	8	11	13	14	3	3	1	0	59
1964	0	0	1	4	2	7	9	17	6	0	3	2	51
1965	1	1	5	2	3	13	21	11	2	2	1	0	62
1966	0	1	1	1	14	9	10	11	17	1	0	0	65
1967	0	1	1	0	2	21	23	9	7	1	0	2	67
1968	1	1	2	3	7	12	10	11	6	11	0	0	64
1969	0	1	3	5	8	10	19	18	9	3	1	1	78
1970	0	2	4	1	1	9	15	11	9	2	0	1	55
1971	0	4	4	1	5	20	19	11	6	13	3	1	87
1972	4	3	5	3	10	8	11	17	1	5	3	1	71
1973	1	0	4	4	7	9	13	11	10	1	1	1	62
1974	0	0	3	3	10	16	21	15	12	3	1	1	85
1975	0	0	2	2	10	21	15	18	15	5	0	0	88
1976	0	0	4	0	17	10	19	10	14	1	0	2	77
1977	2	1	1	1	10	13	17	15	12	3	2	3	80
1978	2	0	1	2	8	12	24	6	8	3	1	1	68
1979	1	2	2	1	11	13	16	15	10	2	1	0	74
1980	2	1	0	4	8	13	13	7	9	4	1	0	62
1981	0	2	1	1	5	7	14	14	8	2	0	3	57
1982	1	2	3	6	7	14	17	16	8	1	3	3	81
1983	2	4	4	3	4	13	13	17	8	7	1	6	82
1984	2	3	1	4	6	9	11	10	5	0	3	1	55
1985	0	0	1	4	9	14	13	19	11	10	1	1	83
1986	2	2	4	0	5	16	15	16	7	4	2	1	74
1987	1	3	7	2	5	10	15	10	13	0	5	0	71
1988	1	0	2	2	5	6	13	15	5	2	1	1	53
1989	1	2	3	6	7	17	15	11	9	5	1	0	77
NOBS	1,013	924	1,009	990	1,023	990	1,023	1,023	990	1,023	990	1,023	12,021
N TSTRMS	27	45	91	85	236	410	496	441	286	112	39	35	2,303
PERCENT	2.7	4.9	9.0	8.6	23.1	41.4	48.5	43.1	28.9	10.9	3.9	3.4	19.2

TABLE 9.3 Percentage Frequency of Thunderstorms at KSC, During the Day, for Each Month.

HOUR (EST)	1	2	3	4	5	6	7	8	9	10	11	12
0	0.0	0.1	0.5	0.6	0.7	0.9	1.2	2.2	2.6	0.8	0.2	0.1
1	0.1	0.2	0.6	0.4	0.7	0.6	1.1	1.3	2.4	1.4	0.1	0.0
2	0.4	0.0	0.8	0.3	0.7	0.9	0.7	0.7	1.6	1.1	0.3	0.0
3	0.1	0.2	1.0	0.1	0.4	0.9	0.2	0.9	1.3	0.9	0.4	0.1
4	0.3	0.3	0.8	0.2	0.7	1.0	0.6	0.9	1.6	1.1	0.3	0.3
5	0.3	0.3	1.2	0.2	0.4	0.5	0.9	0.5	1.0	0.8	0.2	0.1
6	0.0	0.3	0.7	0.1	0.3	0.8	0.4	1.2	1.3	0.5	0.2	0.1
7	0.0	0.1	0.8	0.3	0.3	0.5	1.4	1.0	1.2	0.5	0.3	0.0
8	0.1	0.1	0.6	0.4	0.3	0.5	1.3	0.8	0.8	0.7	0.2	0.0
9	0.3	0.2	0.6	0.2	0.5	0.5	0.9	1.3	1.2	0.4	0.3	0.2
10	0.2	0.3	0.8	0.5	1.0	1.0	1.0	1.2	2.4	0.3	0.3	0.3
11	0.2	0.5	0.8	0.8	1.8	2.9	2.5	4.1	2.4	0.4	0.2	0.0
12	0.2	0.4	1.2	1.2	3.2	5.0	6.6	5.8	2.2	1.2	0.4	0.5
13	0.1	0.8	1.1	1.7	3.7	9.1	11.7	8.5	4.9	1.1	0.6	0.6
14	0.1	0.3	1.2	1.9	5.3	12.8	17.0	14.0	7.0	1.2	0.5	0.3
15	0.2	0.8	0.8	1.9	5.8	14.0	19.1	16.8	7.6	1.9	0.6	0.7
16	0.3	0.5	1.0	1.8	6.3	14.9	19.5	16.2	6.9	2.2	0.6	0.5
17	0.1	0.6	0.8	1.8	7.4	13.6	18.8	14.0	7.4	1.8	0.6	0.9
18	0.2	0.2	1.3	1.2	7.1	11.4	15.5	12.0	6.4	2.3	0.8	0.5
19	0.4	0.4	1.6	1.4	5.3	8.6	10.7	6.3	6.1	2.5	0.3	0.2
20	0.4	0.6	1.2	1.0	4.6	6.4	6.5	5.6	4.8	1.9	0.5	0.1
21	0.0	0.6	1.1	0.8	3.3	4.3	4.9	3.6	3.8	1.1	0.6	0.1
22	0.1	0.4	0.9	0.9	1.6	2.6	2.6	2.2	3.0	0.9	0.4	0.2
23	0.2	0.4	0.7	0.6	1.4	1.6	2.2	1.9	1.9	0.8	0.3	0.0
NOBS	24,265	22,175	24,190	23,756	24,548	23,758	24,550	24,548	23,758	24,550	23,756	24,539
NTSTRMS	43	84	221	203	640	1,144	1,504	1,255	812	281	92	58
PCT	0.2	0.4	0.9	0.9	2.6	4.8	6.1	5.1	3.4	1.1	0.4	0.2

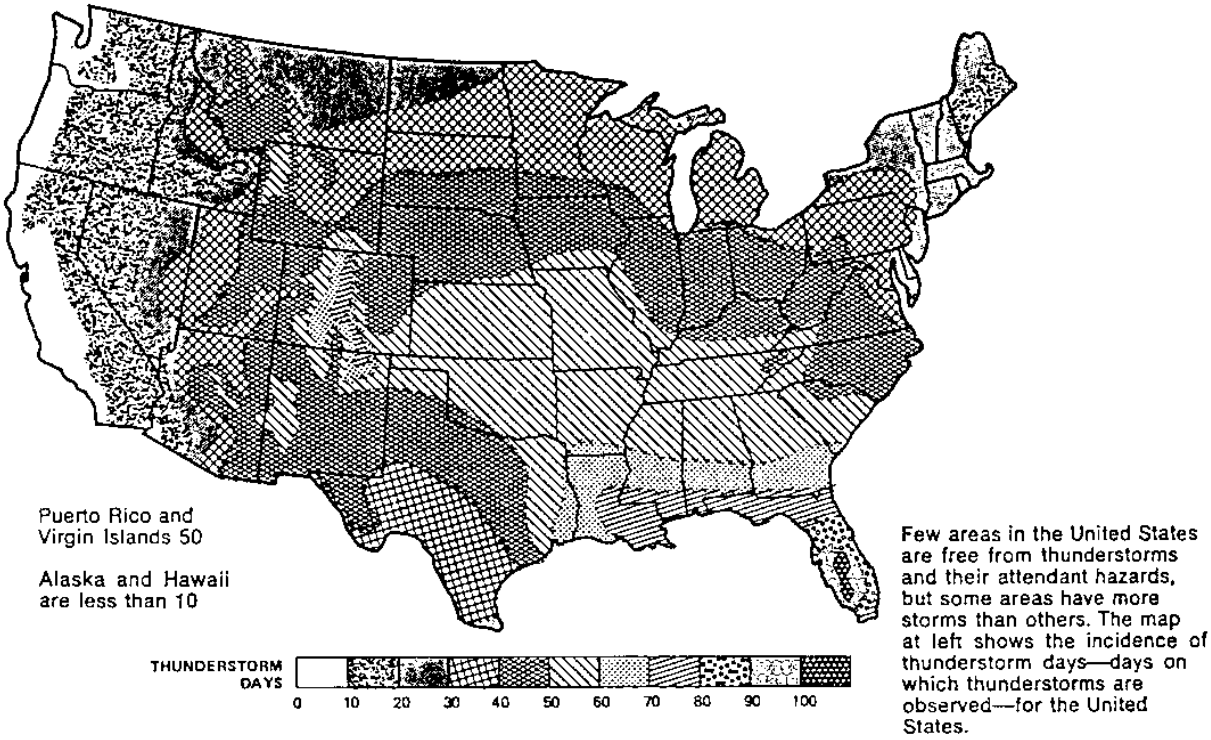

FIGURE 9.4 Incidence of Thunderstorm Days, Per Year (Ref. 9.17).

9.4.1 Characteristics of Cloud-to-Ground Discharges. As shown in figure 9.5, a cloud-to-ground lightning begins in the cloud with a preliminary breakdown process that is not well understood. There seems to be fairly good agreement, however, that this process takes place at roughly the 0 °C to –20 °C level in the cloud, in the region from which negative charge is eventually lowered to ground. This initial breakdown is followed by the stepped leader process that lowers negative charge to ground in a series of steps that typically last 1 μs and are each about 50 m in length. As the stepped leader approaches the Earth, the fields near exposed objects on the ground may become large enough that one or more upward discharges are initiated. This begins the attachment process. One or more of the upward connecting discharges will move up to intersect the stepped leader channel, usually a few tens of meters above the ground. The distance between the tip of the stepped leader and the object about to be struck, at the time when the connecting discharge is initiated is referred to as the striking distance and is an important parameter in lightning protection design.

When contact between the stepped leader and the connecting discharge occurs, the first return stroke is initiated; this high-current breakdown wave effectively carries ground potential upward at roughly 1/3 the speed of light. If additional charge is made available in the cloud by J and K processes, a dart leader may propagate down the residual first return stroke channel. Once electrical connection is made between the dart leader and the ground, a second return stroke is possible (second, third, etc., return strokes are collectively referred to as subsequent strokes). Currents that follow return strokes and that persist for up to several hundreds of milliseconds are sometimes observed and are called continuing currents. Table 9.4 summarizes the important physical characteristics of (negative) cloud-to-ground discharges, i.e., those that bring negative charge to Earth as described above.

9.4.2 Lightning Current Damage Parameters. There are several lightning current parameters that are important in assessing the potential for lightning damage: the peak current, i; the peak current derivative, di/dt; the charge transfer (the integral of current over time), Q; and the action integral (the integral of the square of the current over time), $\int i^2 dt$.

For objects that have primarily a resistive impedance, the peak voltage that develops across the object will depend on the peak current. A large voltage that develops at one end or across an object may lead to discharges through the air and around the object (creating a short circuit) or from the object to ground.

For objects and systems that consist primarily of an inductive impedance, such as cabling in electronics systems or electrical connections on printed circuit cards, the peak voltage will be proportional to the time derivative of the current. For example, if a current with a peak di/dt of 1 kA/μs (one hundredth of a typical lightning peak di/dt value) is injected into a straight length of wire with an inductance of 1 μH/m, a voltage of 1,000 V will develop across 1 m of the wire. It is easy to imagine the damage this could produce in solid-state electronic systems that are sensitive to transient voltages in the tens-of-volts range.

The heating or burn-through of metal sheets such as airplane wings or metal roofs is, to a crude approximation, proportional to the charge transferred during a lightning strike. Generally, large charge transfers occur during the long-duration, low-current amplitude portions of lightning discharges such as the continuing current phase, rather than during the short-duration, high-current amplitude return stroke processes.

The heating of electrically conducting materials and the explosion of non-conducting objects is, to a first approximation, determined by the value of the action integral since the quantity $\int i^2 R dt$ is the Joule heating (R is the resistive impedance). Generally, electrical heating vaporizes internal material, and the resulting increase in pressure causes a fracture or explosion to occur.

9.4.3 Tower Measurements of Current. Table 9.5 summarizes typical lightning current parameter values obtained from tower measurements performed atop Mt. San Salvatore in Switzerland (9.22). The data in parentheses are from tower measurements conducted in Italy (9.23).

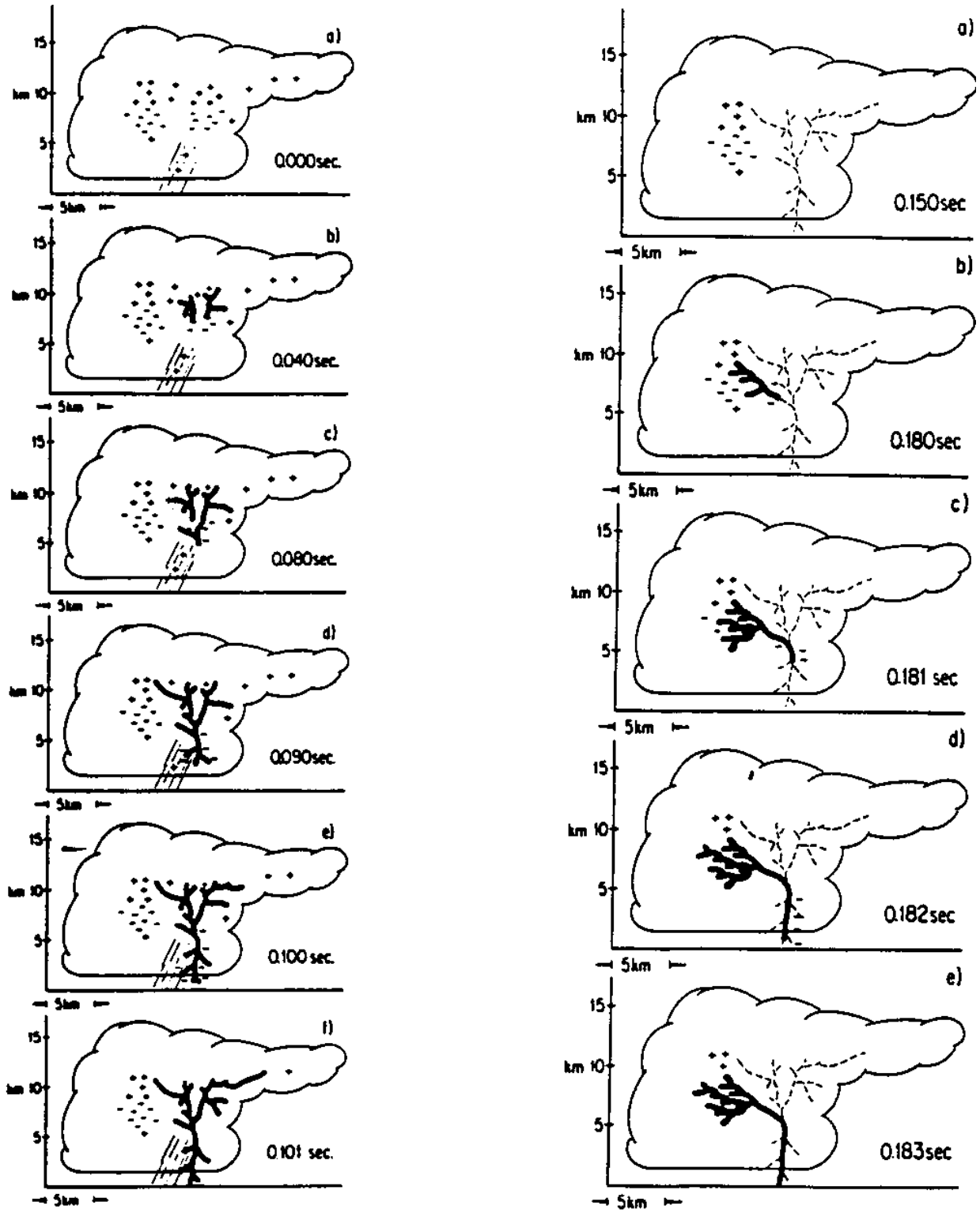

FIGURE 9.5. First Column is a Sketch of the Luminous Processes that Form the Stepped Leader and the First Return Stroke in a Cloud-To-Ground Lightning Flash. Second Column Shows the Development of a Lightning Dart-Leader and a Return Stroke Subsequent to the First in a Cloud-to-Ground Lightning (Ref. 9.22).

TABLE 9.4 Typical Negative Cloud-to-Ground Lightning Characteristics (Adapted from Ref. 9.10).

Cloud-to-Ground Flash	
Number of return strokes	3 to 4
Time between return strokes	50 ms
Duration of flash	0.5 s
Charge transferred	25 C
Stepped Leader	
Duration	10 to 30 ms
Step length	50 m
Step interval time	50 μs
Average velocity	1 to $2x10^5$ m/s
Step velocity	$>5x10^7$ m/s
Charge lowered	10 C
Average current	100 to 1,000 A
Peak step current	≥ 1 kA
Upward Discharge	
Length	10 to 20 m (above flat terrain) 20 to 100 m (above tall structures)
First Return Stroke	
Peak current	10 to 30 kA
Peak current rate of rise	100 kA/μs
Velocity	$1x10^8$ m/s
Dart Leader	
Duration	2 ms
Average velocity	0.5 to $1x10^7$ m/s
Charge lowered	1 C
Average current	1 kA
Dart-Stepped Leader	
Step length	10 m
Step interval time	10 μs
Average velocity	$1x10^6$ m/s
Subsequent Return Strokes	
Peak current	10 kA
Current rate of rise	100 kA/μs
Velocity	$1x10^8$ m/s
Continuing Current	
Duration	0.1 s
Current	100 to 300 A
Charge transfer	10 C

TABLE 9.5 Negative Cloud-to-Ground Lightning Current Parameters Measured in Strikes to Instrumented Towers (Refs. 9.22 And 9.23).

Parameter (Units)	Number Events	Percentage of Cases Exceeding Tabulated Value 95%	50%	5%
Peak Current (kA)				
First Strokes	101	4	30	80
	(42)		33	
Subsequent Strokes	135	4.6	12	30
	(33)		(18)	
Peak DI/dt (kA/μs)				
First strokes	92	5.5	12	32
	(42)		(14)	
Subsequent strokes	122	12	40	120
	(33)		(33)	
Charge (C)				
First strokes	93	1.1	5.2	24
Subsequent strokes	122	0.2	1.4	11
Flash (all strokes)	94	1.3	7.5	40
Action Integral (A^2 s)				
First strokes	91	6.0×10^3	5.5×10^4	5.5×10^5
Subsequent strokes	88	5.5×10^2	6.0×10^3	5.2×10^4
Front Duration (μs)*				
First strokes	89	1.8	5.5	18
	(42)		(9)	
Subsequent strokes	118	0.22	1.1	4.5
	(33)		(1.1)	
Stroke Duration (μs)**				
First strokes	90	30	75	200
	(42)		(56)	
Subsequent strokes	115	6.5	32	140
	(33)		(28)	
Time Between Strokes (ms)	133	7	33	150
Flash Duration				
(including single stroke flashes)	94	0.15	13	1,100
(excluding single stroke flashes)	39	31	180	900

Notes:
*2 kA to peak
**2 kA to half-peak amplitude value

9.4.4 Triggered Lightning Current Measurements. It is often argued that triggered lightning realistically simulates natural lightning and may be used in studies of lightning physics and lightning protection technology. The first successful attempts to trigger lightning over land were performed at the St. Privat d'Allier station in south-central France. In this and similar experiments that followed, a small antihail rocket, approximately 85-cm tall and weighing 2.7 kg, was fired upward into a thundercloud and carried a wire that unspooled from the ground. The rocket developed a maximum speed of about 200 m/s and could reach an altitude of about 700 m in 5 s. Cotton-covered steel wire (0.18-mm diameter) was used. An upward leader was initiated from the top of the rocket when the rocket had reached an altitude of typically 200 to 300 m. A triggering attempt was generally successful if the static field at the ground was equal to or greater than 10 kV/m, though success also depended on the storm and on the amount of natural lightning activity. Rocket heights at the time of initiation were between 50 and 530 m with a mean of 210 m. Fields at the time of successful launches ranged from –6 to –17 kV/m with a mean of 10 kV/m.

Since the initial experiments at St. Privat d'Allier in France, additional experiments have been performed in Japan, New Mexico, and Florida. The results of these experiments are summarized in table 9.6. Note that the four basic lightning current "damage parameters" discussed above are included in the table. These data represent the best estimates of natural lightning peak *di/dt* amplitudes available at the present time.

9.4.5 Inferring Damage Parameters From Lightning Fields. Aside from measuring lightning current parameters directly from tower strikes as sited above, one can infer values of the current and current derivative from measurements of the radiated fields. The variety of discharge processes which occur during a lightning flash generate electromagnetic radiation over a very broad range of frequencies ranging from near dc to microwave band. A variety of lightning processes including leaders, certain intracloud discharges, and return strokes all produce large-amplitude radiation field changes in a fraction of a microsecond. Abruptly changing fields have important implications in the design of lightning protection equipment and are also of interest because they imply large and rapid current variations.

It is only in about the last 10 years that accurate measurements of the fastest lightning field variations have been made. This is due partly to the increased availability of suitable recording equipment. It is due also to the realization that, since high frequency content of lightning fields is degraded by propagation over land, fast-field changes can be adequately observed only if the propagation path from the lightning to the recording station is entirely over salt water.

Figure 9.6 is a schematic representation of simultaneous photographic and electric field measurements for a multiple-stroke, cloud-to-ground lightning flash. This will serve to illustrate typical lightning field variations in different frequency intervals and on different time scales.

Electric field variations below a few tens of megahertz are commonly measured using broadband antenna systems. The sensing element is often a flat conductor which is placed horizontally on the Earth's surface (e.g., 9.24). A current flows to and from the antenna in response to a changing external electric field. The antenna current is then integrated to give an output voltage proportional to *E*. In "slow antenna" systems, an amplifier decay time constant of several seconds is used. This is several times longer than the duration of the flash, and an accurate record of the entire field change is obtained. "Fast antenna" systems have a shorter decay time constant, typically hundreds of microseconds, so that the amplifier output voltage will recover to near zero between separate events. In this way, the structure of each impulsive component within a discharge can be studied with the full dynamic range of the amplifier.

Note that the schematic slow *E*-field record is dominated by large transitions produced by the separate return strokes. More slowly varying fields, representing charge transport occurring during leader processes and continuing currents are also detected with slow antenna systems.

TABLE 9.6 Mean Lightning Current Parameters for Rocket-Triggered Lightning Events.*

Parameter (units)	Number of Events	Percentage of Cases Exceeding Tabulated Value 90%	50%	10%	Maximum Value
Peak Current (kA)					
France (a)	94	2	12	29	42
New Mexico (a)	35	4	18	30	40
Florida (1985–1988)	231	5.5	12	26	60
France (1986)	9		13		48
Peak dI/dt (kA/μs)					
Florida (1985)	31	61	102	171	250
Florida (1987, 1988)	74	42	125	215	411
France (1986)	9		78		139
Charge (C) Per Stroke	35		0.35 (b)		
New Mexico			0.95 (c)		
Charge (C) Per Flash					
France	94	4	50	100	140
New Mexico	35	6	35	175	
Action Integral (A^2 s)					
France	94	$3x10^2$	$6x10^3$	$5x10^4$	$3x10^5$
Flash Duration (ms)					
France	94	70	350	850	1,300
New Mexico	35	250	470	940	
Percentage of Flashes with only a Continuous Current Phase		France	40%		
		New Mexico	20%		
Number of Pulses Per Flash					
New Mexico (b)	94	4	350	11	53
	35		470	10 (b)	

Notes:
(a) Distribution of only the largest peak current in each flash.
(b) Only pulses with peak currents ≥ 3 kA were included.
(c) Only pulses with peak currents ≥ 10 kA were included.

*This table is from data found in Refs. 9.40 through 9.46.

The fine structure of large amplitude fast *E*-field impulses is shown on expanded time scales below the fast *E*-field record in figure 9.6. These highly time-resolved *E*-field signatures are complicated by a variety of discharge processes. At the bottom of figure 9.6 is a schematic depiction of VHF lightning radiation such as would be detected using a tuned, narrowband receiver. Radiation at these frequencies is currently being used in time-of-arrival and interferometric systems to locate and follow lightning channel growth and propagation in thunderstorm clouds.

To infer lightning current and current derivative from the radiated fields, one begins by considering the fields emitted by a straight, vertical current element of length *H* above a perfectly conducting ground (9.25). The geometry for this calculation is given in figure 9.7. At the ground, at a distance D from the ground-strike point, the field in MKS units is given by:

$$\vec{E}_{\text{total}} = \frac{1}{2\pi\varepsilon_0}\int_0^H (E_R+E_I+E_S)\, dz'\,\hat{z}\ , \tag{9.2}$$

where

$$E_R = -\frac{\sin^2\alpha}{c^2R}\frac{\partial i}{\partial t}(z',t-R/c) = \text{radiation term}$$

$$E_I = \frac{(2-3\sin^2\alpha)}{cR^2}\, i(z',t-R/c) = \text{induction term}$$

$$E_S = \frac{(2-3\sin^2\alpha)}{R^3}\int_0^t i(z',\tau-R/c)\, d\tau = \text{electrostatic term}\ .$$

where ε_0 is the permitivity of free space.

The radiation or “far-field” component decays more slowly with distance than the other components and thus becomes dominant at large distances.

It is not possible to solve equation (9.2) for the current in terms of measured electric fields. Rather, it is necessary to assume a functional form for the channel current (a function of time and channel height). If it is possible to adjust current model parameters until good agreement with measured fields and the observed wave front speed is obtained, then the model current is assumed to be a realistic approximation to the true current. A realistic current model would be of practical importance because (1) return stroke currents and statistical distributions of current parameters could be determined from remote measurements of lightning fields, and (2) realistic fields could be calculated for use in “coupling” calculations, such as might be used to determine voltages induced on power lines from a nearby lightning strike.

The model most widely used to derive lightning currents from measured fields is the transmission-line (TL) model (9.26). The TL model assumes that the current which is measured at the ground propagates up the channel at a constant velocity, without distortion, much as it would along a lossless transmission line. The TL model current has the following functional dependence:

$$\begin{aligned} i(z',t) &= i(0,t-z'/v) \quad z' \le L(t) \\ i(z',t) &= 0 \qquad\qquad z' > L(t)\ . \end{aligned} \tag{9.3}$$

Here, $L(t)$ is the height of the return stroke wavefront at time *t*. A particularly simple relationship between the currents and the radiation belts, at a distance *r*, is obtained for the TL model current:

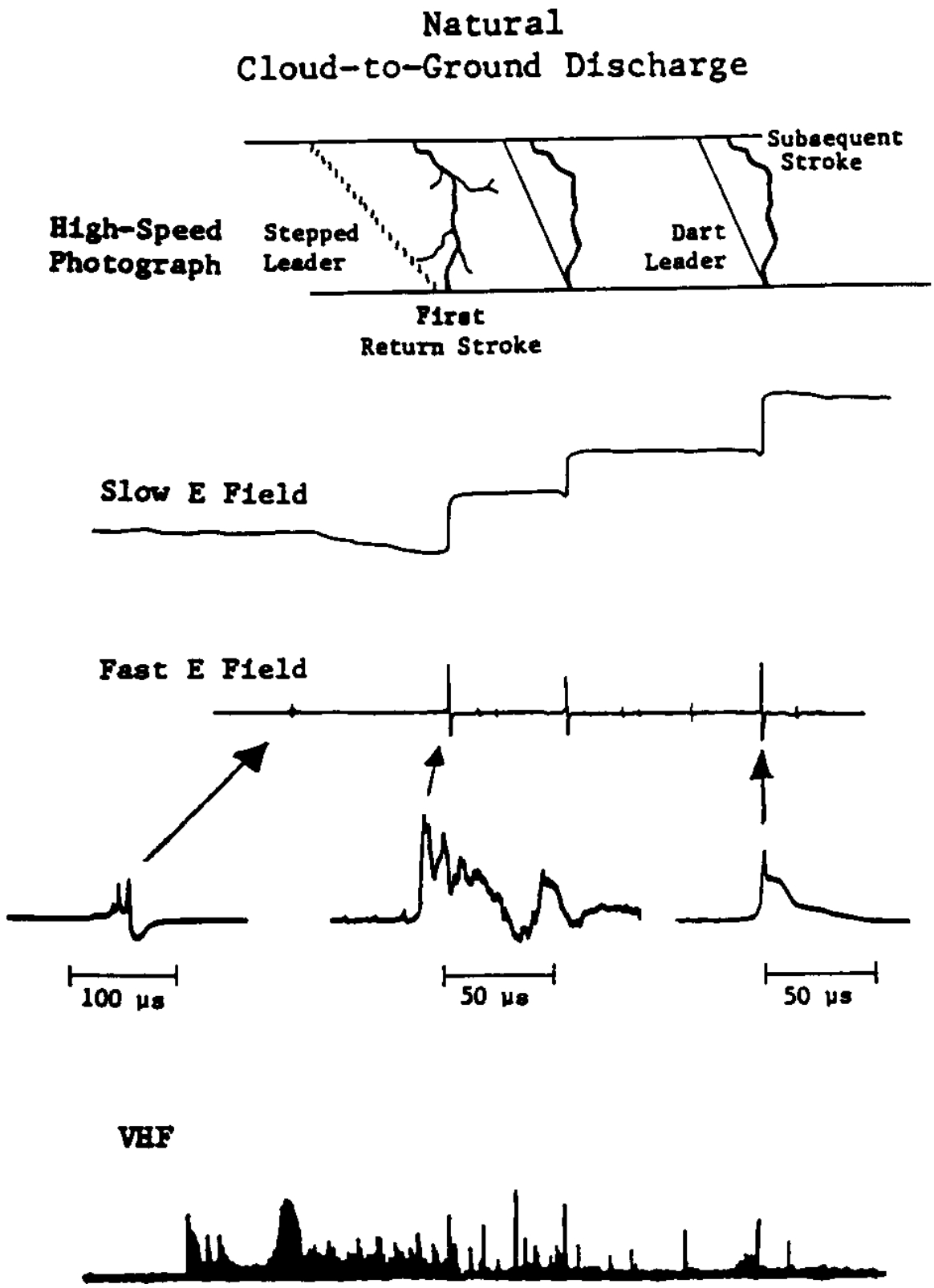

FIGURE 9.6 Simultaneous Photographic and Electric Field Measurements for a Multiple Stroke, Cloud-To-Ground Lightning Flash. The Schematic at the Bottom is an Example of a VHF Lightning Radiation Signature (Adapted From Ref. 9.10).

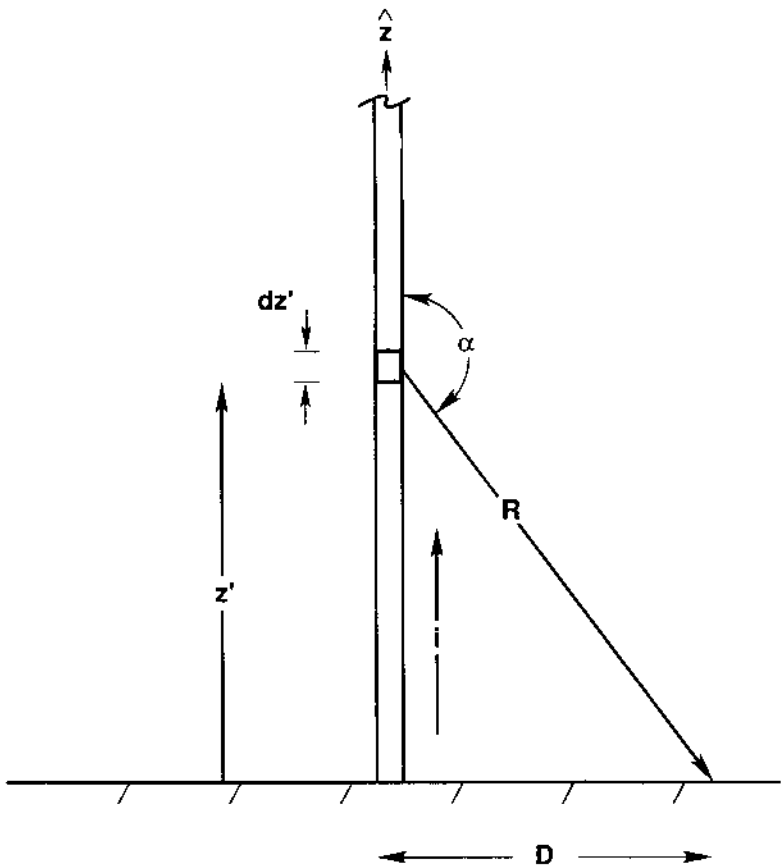

FIGURE 9.7 Geometry Used to Infer Lightning Current Characteristics from the Radiated Field (Ref. 9.25).

$$i(t) = \frac{2\pi\varepsilon_0 c^2 r}{v} E_R(r,t+r/c)$$

$$\frac{di}{dt}(t) = \frac{2\pi\varepsilon_0 c^2 r}{v} \frac{dE_R}{dt}(r,t+r/c) \ . \tag{9.4}$$

These equations are the basis for field-inferred current parameters. In the TL model, since the same current wave shape passes all points on the channel, charge is only transferred from the bottom of the channel to the top, and the leader channel is not discharged. There is poor agreement, therefore, between model and measured fields at longer times. In practice, these relations are applied at or before the time of peak return stroke current. Typical value of peak field derivative for cloud-to-ground return strokes is about 40 V/m/μs.

9.5 Lightning Test Standards. In this section we will review lightning current standards that have recently been adopted for the design and verification of lightning protection for aerospace vehicles. The aerospace industry has generally kept better pace with advancements in our understanding of lightning processes and changes in vehicle design than has been the case for most ground-based systems. Reviews of lightning test standards used in the aerospace industry have been given by Reference 9.27. A discussion of lightning protection techniques is beyond the scope of this report. A comprehensive treatment of lightning protection of aircraft may be found in reference 9.28.

9.5.1 Historical Perspective. The first airplane lightning protection test standards were published in the mid-1950's by the Federal Aviation Administration (FAA) (Ref. 9.29) and the U.S. Department of Defense (DOD) (9.30). MIL-B-5087 dealt exclusively with the electrical bonding of aircraft components. Bonding refers to a low-resistance electrical connection between components that is sufficient to withstand lightning currents. At the time, it was generally believed that the damaging effects of lightning were limited to the exterior of the aircraft or structures directly exposed to a lightning strike (see 9.31 for a review of the direct effects of lightning). It was felt that sufficient protection would be provided if these components were adequately bonded to the main air frame. The FAA circular dealt exclusively with the protection of aircraft fuel systems.

Two spectacular incidents in the 1960's indicated clearly that other lightning related effects could lead to catastrophic accidents. On December 8, 1963, a lightning strike ignited fuel in the reserve tank of a Boeing 707 commercial airliner. The left wing of the aircraft was destroyed and 81 people on board were killed. In 1969, Apollo 12 was launched into clouds that had not been producing lightning. The Saturn V rocket artificially triggered two discharges. The lightning strikes produced major system upsets, but only minor permanent damage and the vehicle and crew survived and were able to complete their mission (Ref. 9.1). These and accidents motivated the FAA and the DOD to request that the Society of Automotive Engineers (SAE) committee on electromagnetic compatibility (SAE-AE4) formulate improved lightning protection design and test standards. The report issued by that group (9.32) quickly became the standard for the U.S. civil aviation industry. A revision of that report followed in 1978 (Ref. 9.33). The 1978 report, given a blue cover, became known as the "blue book" and was adopted for both civil and military aircraft and by foreign certification agencies. The SAE defined lightning environment was formally incorporated into military protection specifications in MIL-STD-1757 (Ref. 9.34), and a revision MIL-STD-1757A (Ref. 9.35), and by the FAA in advisory circular 20-53A (Ref. 9.36).

A panel was also convened in the early 1970's to formulate lightning protection standards for the NASA space shuttle program. The result of that activity was the publication of the "Shuttle Lightning Protection Criteria Document," NSTS-07636 (Ref. 9.37). The lightning environment defined in that document predated and differed somewhat from that in the SAE 1978 report, but the key aspects of the current test waveforms were nearly the same.

Several more recent trends in the design of aerospace vehicles have resulted in an increased vulnerability to the indirect effects of lightning. These developments include the use of nonmetallic, lightweight, composite materials in the skin and structure of the vehicle which do not shield the interior of the aircraft as efficiently as a metal body, and an increased reliance on digital flight control electronics as opposed to analog and mechanical systems. In these cases, the lightning damage occurs not as a direct result of the lightning currents, but from spurious signals that are induced or coupled into the interior of the vehicle where they may damage or upset electronic processing equipment (Ref. 9.38). A recent example of the hazards associated with indirect lightning effects is provided by the Atlas/Centaur accident which occurred in March 1987 (Ref. 9.3). Investigation of that incident determined that the vehicle was struck by a triggered cloud-to-ground flash. The lightning current caused a transient signal to be coupled into the Centaur digital computer unit where data in a single memory location was changed. The computer

subsequently issued an erroneous yaw command which resulted in large dynamic stresses being placed on the vehicle and caused the vehicle to breakup.
Indirect lightning hazards have required additional changes in protection design philosophy. Also, in an effort to better evaluate the lightning hazards, new research programs were undertaken in the 1980's by NASA, the U.S. Air Force, the FAA, and the French Government. Experimental results from these studies have been incorporated into the most recent aerospace vehicle lightning standards (Refs. 9.4, 9.5, 9.39).

9.5.2 Severe Direct Lightning Strike Current Test Waveforms. Five current component waveforms which would represent a severe lightning strike event are specified in the SAE 1987 report (Ref. 9.5) which is the industry standard for transport aircraft. The SAE 1987 test specifications have also been incorporated into a recent revision of the "Shuttle Lightning Protection Criteria Document" (Ref. 9.4). The SAE 1987 current waveforms are illustrated in Figure 9.8 and consist of:

Component A

This waveform represents a first return stroke with a peak current of 200 kA, and is defined mathematically by:

$$I(t) = I_o(e^{-at} - e^{-bt}) \ , \tag{9.5}$$

where I_o is 218,810 A, a = 11,354 s^{-1}, b = 647,265 s^{-1}, and t is time in seconds. This waveform component has a very large peak current, peak current derivative, and action integral.

Component B

This component represents an intermediate current following the first return stroke. Component B has an average amplitude of 2 kA and transfers 10 C of charge. This component is described by a double exponential of the form shown in equation (9.5) with I_o = 11,300 A, a = 700 s^{-1}, and b = 2,000 s^{-1}.

Component C

This waveform represents a continuing current. Component C is a square waveform with a current amplitude between 200 and 800 A and a duration of 1 to 0.25 s chosen to give a total charge transfer of 200 C. The primary purpose of this waveform is charge transfer.

Component D

Component D represents a subsequent stroke with a peak current of 100 kA. This component is described by a double exponential of the form shown in equation (9.5) with I_o = 109,405 A, a = 22,708 s^{-1}, and b = 1,294,530 s^{-1}.

Component H

Component H is a short duration, high rate of rise current pulse with a peak current amplitude of 10 kA. This test waveform incorporates important characteristics of lightning discharges recorded during triggered strikes to instrumented aircraft in flight. This waveform is also defined by a double exponential with I_o = 10,572 A, a = 187,191 s^{-1}, and b = 19,105 s^{-1}. Component H has a peak current derivative of 2×10^{11} A/s.

Figure 9.9 depicts and lists the key aspects of a current waveform consisting of the sum of components A, B, C, and D. The test values, a peak current of 200 kA, a charge transfer of 200 C, and an action integral of $2x10^6$ A^2 s, occur at the 1-percent level or less in negative ground discharges. Approximately 10 percent of positive ground discharges, however, while generally more infrequent, would be expected to exceed these test values. The peak current derivative test value, $1.4x10^{11}$ kA/μs, probably does not represent a severe level test. Referring back to table 9.6, we note that 10 percent of the return strokes triggered in Florida during 1987 and 1988 had current derivatives which exceeded 215 kA/μs. A maximum peak *dI/dt* value of 411 kA/μs has been measured in Florida, for a stroke with a peak current of about 60 kA, and a *dI/dt* value of 380 kA/μs was recorded during measurements conducted with the NASA F-106 aircraft.

A typical ground flash consists of a first return stroke followed by several subsequent strokes. For protection against direct effects, it is adequate to consider only one return stroke (component A or D). For a proper evaluation of indirect effects, such as coupling into the interior of aerospace vehicles, it is necessary to consider the multiple stroke nature of an actual flash. For this purpose, a multiple stroke consisting of a component A current pulse followed by 23 randomly spaced subsequent strokes of 50 kA peak amplitude (component D divided by 2), all occurring within 2 s, has been defined. The multistroke test waveform is illustrated in figure 9.10.

Rapid sequences of pulses with low-peak current amplitude, but large current derivative values, were observed during the lightning strike measurements made with instrumented aircraft. While a single current pulse, like component H, is not likely to cause physical damage, a burst of randomly distributed pulses may cause interference or upset in some systems. A test standard consisting of component H current pulses occurring repetitively, in a 2 s period, in 24 randomly spaced groups of 20 pulses each, has been defined. This multiple burst waveform is illustrated in figure 9.11.

The idealized waveforms described above are appropriate for design analyses. The cost of constructing a simulator capable of delivering these test waveforms to actual vehicles may be prohibitive. In that case, actual testing may involve the use of different waveforms. It must be possible, however, to extrapolate or scale the test results made with the alternate waveforms to the severe hazard level described above.

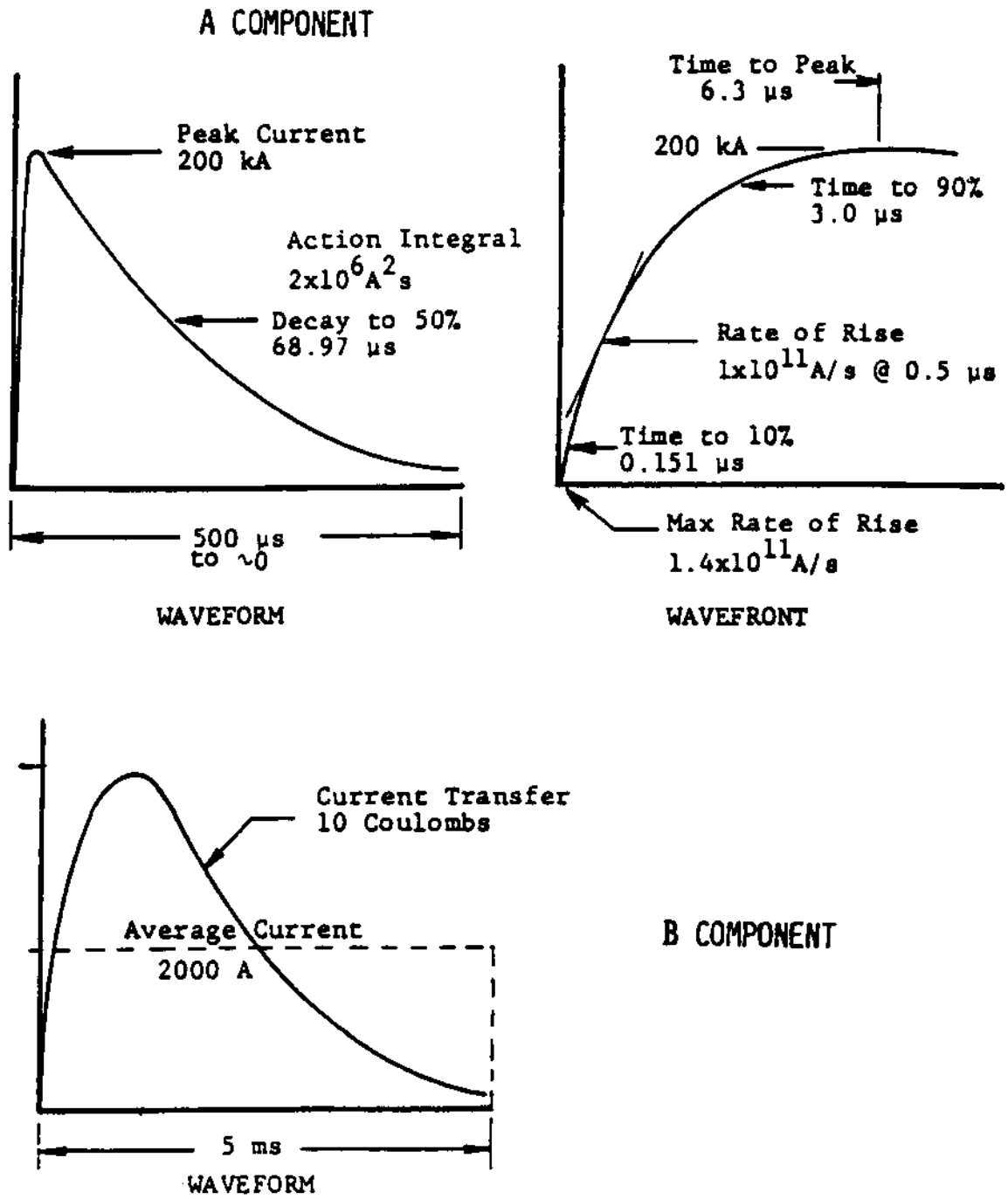

FIGURE 9.8 The SAE 1987 Current Test Waveforms for Severe Direct Lightning Strikes to Aircraft (Ref. 9.5).

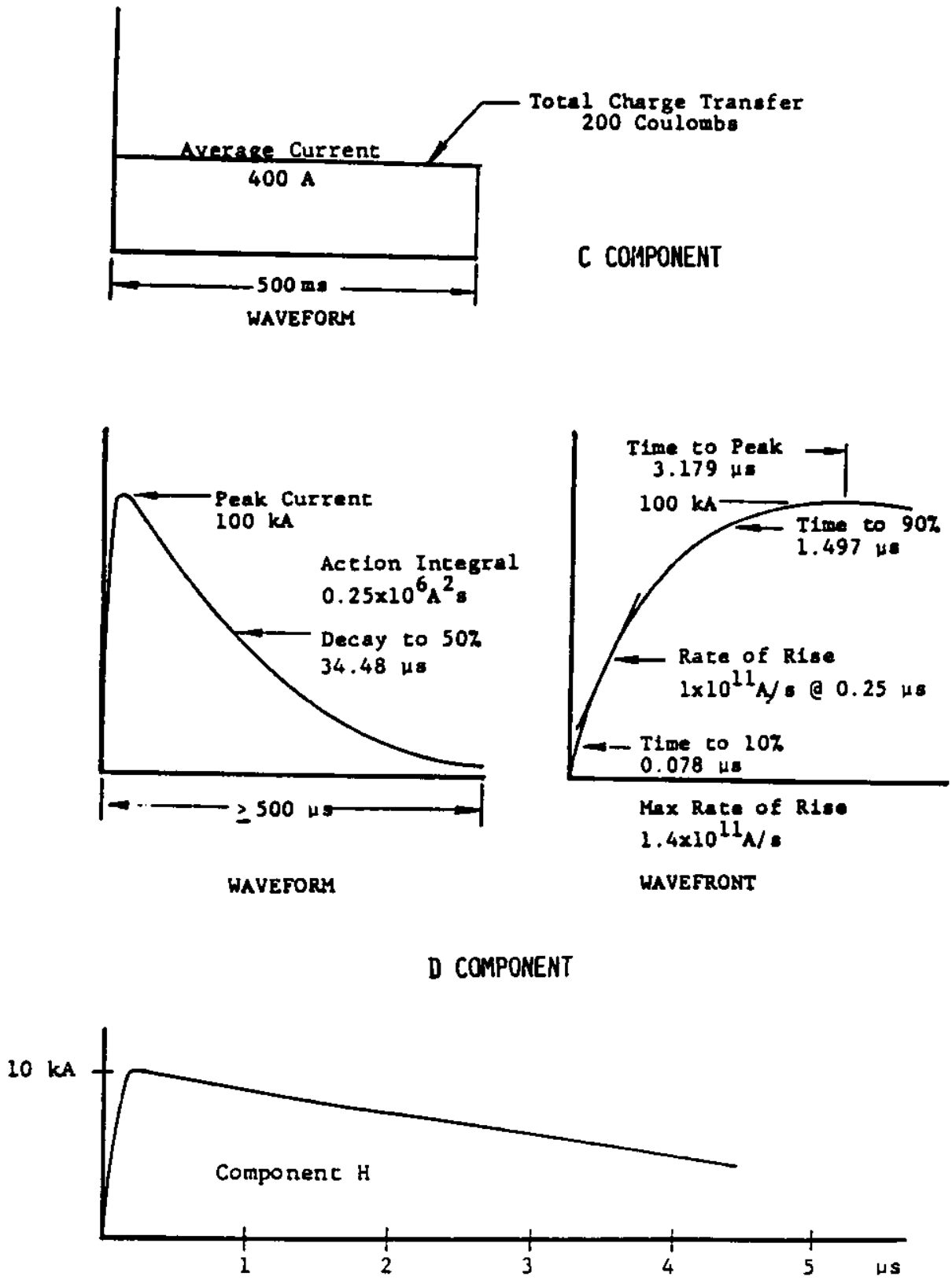

FIGURE 9.8 (Cont'd) The SAE 1987 Current Test Waveforms for Severe Direct Lightning Strikes to Aircraft (Ref. 9.5)

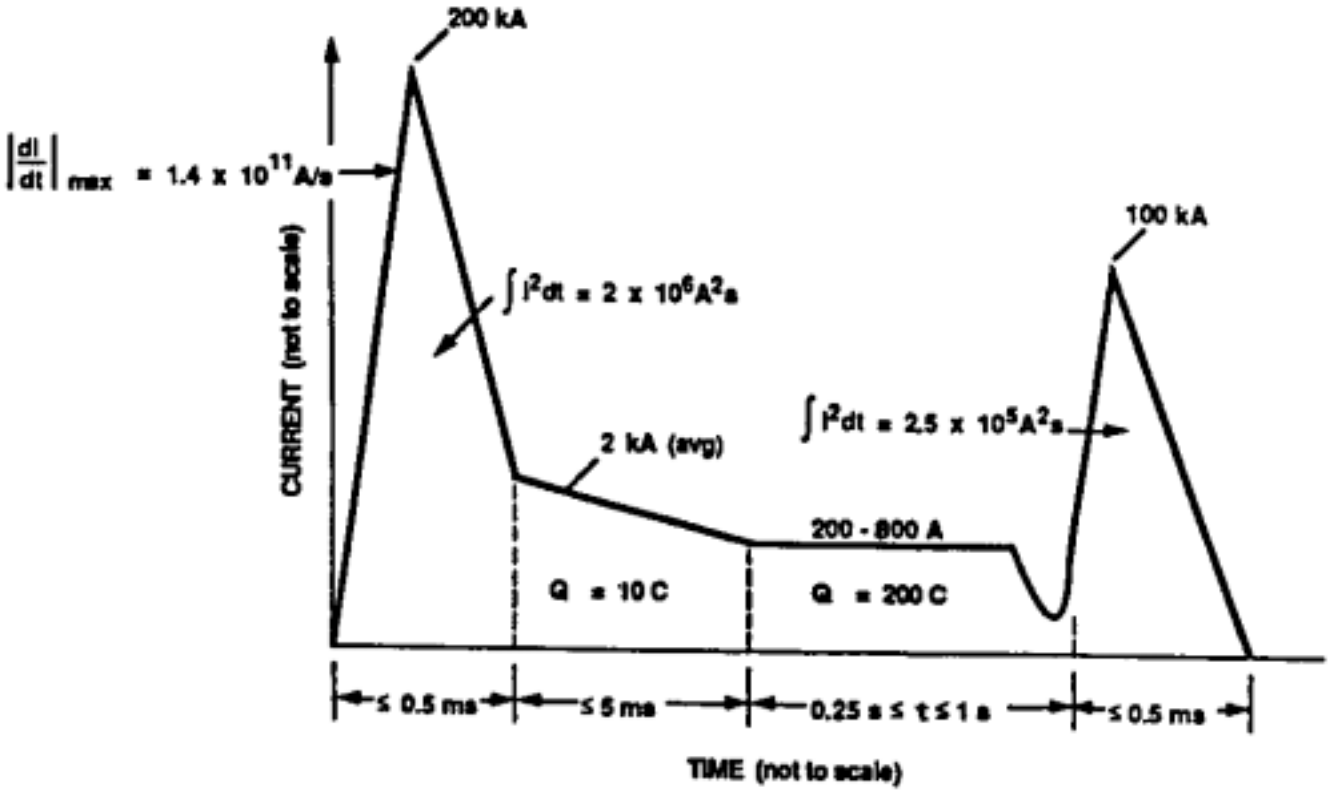

FIGURE 9.9 Current Waveform Composed of the Four Components A, B, C, and D Shown in Figure 9.8 (Ref. 9.5).

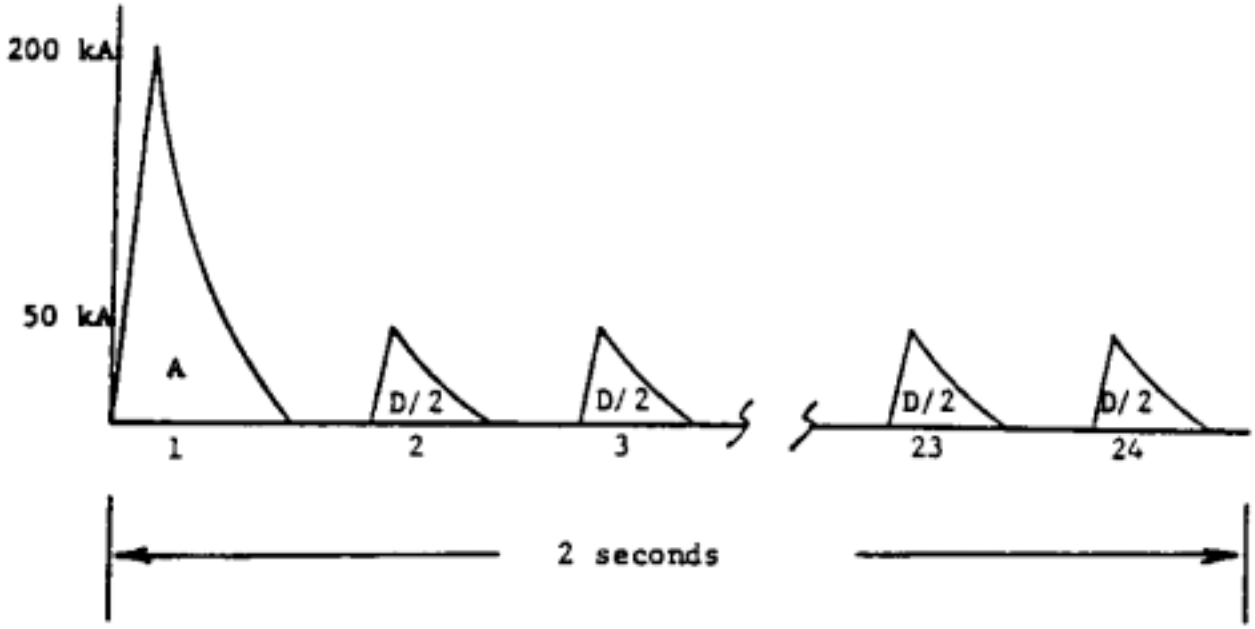

FIGURE 9.10 Multiple Stroke Lightning Current Test Waveform Consisting of a First Stroke (Component A) and Followed by 23 Subsequent Strokes (Attenuated D Components) (Ref. 9.5).

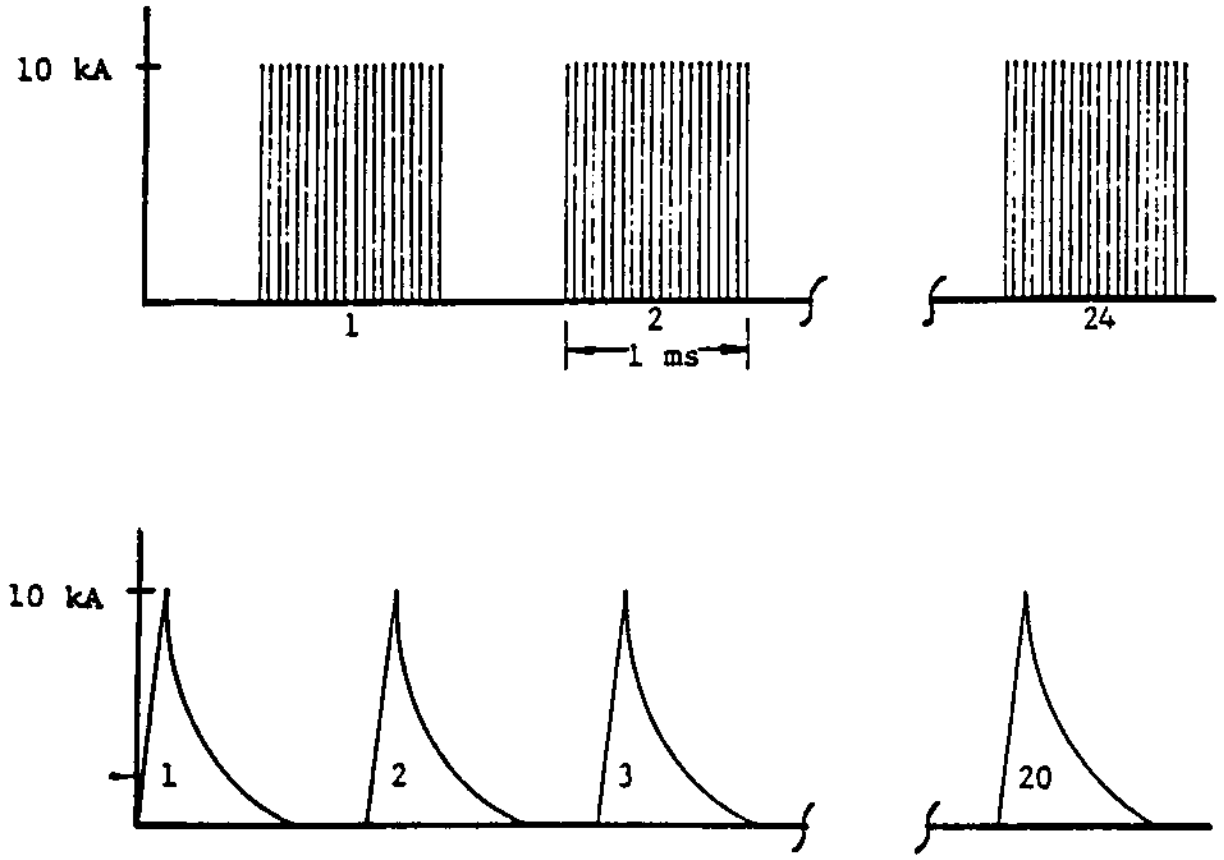

FIGURE 9.11 A Current Test Waveform Composed of 24 Bursts (Top Figure) that are Randomly Spaced Within a 2-s Period. Each Burst (Bottom Figure) Consists of 20 Pulses Randomly Spaced Within a 1-ms Period (Ref. 9.5).

This Page Left Blank Intentionally

REFERENCES

9.1 "Analysis of Apollo 12 Lightning Incident," Document No. MSC-01540, prepared jointly by Marshall Space Flight Center, Kennedy Space Center, and Manned Spacecraft Center, National Aeronautics and Space Administration, February 1970.

9.2 Brook, M., Holmes, C.R., and Moore, C.B.: "Lightning and Rockets—Some Implications of the Apollo 12 Lightning Event." Naval Research Reviews, vol. 23, No. 4, April 1970, pp. 1–17.

9.3 Christian, H.J., Mazur, V., Fisher, B.D., Ruhnke, L.H., Crouch, K., and Perula, R.P.: "The Atlas/Centaur Lightning Strike Incident." J. Geophys Res., vol. 94, 1989, pp. 13169–13177.

9.4 National Aeronautics and Space Administration, "Lightning Protection Criteria Document," NSTS-07636, Revision E., Lyndon B. Johnson Space Center, March 18, 1988.

9.5 Society of Automotive Engineers, Recommended Draft Advisory Circular: "Protection of Aircraft Electrical/Electronic Systems Against the Indirect Effects of Lightning," Report of SAE Committee AE-4L, February 4, 1987.

9.6 Beard, K.V.K., and Ochs, H.T.: "Charging Mechanisms in Clouds and Thunderstorms," in The Earth's Electrical Environment, E.P. Krider and R.G. Roble (eds.), National Academy Press, Washington, DC, 1986, pp. 114–130.

9.7 Lhermitte, R., and Williams, E.: "Cloud Electrification." Rev. Geophys. Space Phys., vol. 21, 1983, pp. 984–992.

9.8 Krehbiel, P.R.: "The Electrical Structure in Thunderstorms," in The Earth's Electrical Environment, E.P. Krider and R.G. Roble (eds.), National Academy Press, Washington, DC, 1986, pp. 90–113.

9.9 Koshak, W.J., and Krider, E.P.: "Analysis of Lightning Field Changes During Active Florida Thunderstorms." J. Geophys. Res., vol. 94, 1989, pp. 1165–1186.

9.10 Uman, M..A.: "The Lightning Discharge." Academic Press, Orlando, Florida, 1987.

9.11 Prentice, S.A.: "The Frequency of Lightning Discharges in Lightning," vol. 1, R.H. Golde (ed.), Academic Press, New York, New York, 1977, pp. 465–495.

9.12 Krider, E.P., Noggle, R.C., and Uman, M.A.: "A Gated Wideband Magnetic Direction Finder for Lightning Return Strokes." J. Appl. Meteorol., vol. 15, 1976, pp. 301–306.

9.13 Christian, H.J., Blakeslee, R.J., and Goodman, S.J.: "The Detection of Lightning From Geostationary Orbit," J. Geophy. Res., vol. 94, 1989, pp. 13329–13337.

9.14 WMO, World Distribution of Thunderstorm Days, Part I: Tables, WMO/OMM—No. 21, TP. 6, World Meteorological Organization, Geneva, 1953. (WMO Publications Center, P.O. Box 433, New York, New York 10016.)

9.15 WMO, World Distribution of Thunderstorm Days, Part II: Tables of Marine Data and World Maps, WMO/OMM—No. 21, TP. 21, World Meteorological Organization, Geneva, 1956.

9.16 Changnon, S.A., Jr.: "Secular Variations in Thunder-Day Frequencies in the Twentieth Century." J. Geophys. Res., vol. 90, 1985, pp. 6181–6194.

9.17a "Thunderstorms and Lightning," NOAA/PA 83001 pamphlet, GPO, 1984.

9.17b Changery, M.J.: "National Thunderstorm Frequencies for the Contiguous United States." NUREG/CR-2252, U.S. Nuclear Regulatory Commission, Washington, DC, November 1981.

9.18 Robinson, P.J., and Easterling, D.R.: "The Frequency Distribution of Thunderstorm Durations." Journal of Applied Meteorology, vol. 27, January 1988.

9.19 Easterling, D.R., and Robinson, P.J.: "The Diurnal Variation of Thunderstorm Activity in the United States." Journal of Climate and Applied Meteorology, vol. 24, October 1985.

9.20 Michaels, P.J., et al.: "Composite Climatology of Florida Summer Thunderstorms." Monthly Weather Review, vol. 115, November 1987.

9.21 Kelly, D.L., and Schaefer, J.T.: "Climatology of Nontornadic Severe Thunderstorm Events in the United States." Monthly Weather Review, vol. 113, No. 11, November 1985.

9.22 Berger, K., Anderson, R.B., and Kroninger, H.: "Parameters of Lightning Flashes." Electra, No. 41, 1975, pp. 23–37.

9.23 Garbagnati, E., and Lo Pipero, G.B.: "Parameter von Blitzstromen." Elektrotech. Z., ETA-A, vol. 103, 1982, pp. 61–65.

9.24 Krider, E.P., Weidman, C.D., and Noggle, R.C.: "The Electric Fields Produced by Lightning Stepped Leaders." J. Geophys. Res., vol. 82, 1977, pp. 951–960.

9.25 Uman, M.A., Brantley, R.D., Tiller, J.A., Lin, Y.T., Krider, E.P., and McLain, D.K.: "Correlated Electric and Magnetic Fields From Lightning Return Strokes." J. Geophys. Res., vol. 80, 1975, pp. 373–376.

9.26 Uman, M.A., and McLain, D.K.: "Lightning Return-Stroke Current From Magnetic and Radiation Field Measurements." J. Geophys. Res., vol. 75, 1970, pp. 5143–5147.

9.27 Clifford, D.W., Crouch, K.W., and Schulte, E.H.: "Lightning Simulation and Testing." IEEE Trans. Electromag. Comp., EMC-24, 1982, pp. 209–224.

9.28 Fisher, F.A., Plumer, J.A., and Perala, R.A.: "Lightning Protection of Aircraft." Lightning Technologies Inc., Pittsfield, Massachusetts, 1990.

9.29 Federal Aviation Administration: "Protection of Aircraft Fuels Systems Against Lightning," U.S. FAA Advisory Circular 25-3, Washington, DC, November 10, 1965.

9.30 U.S. Department of Defense: "Bonding, Electrical, and Lightning Protection for Aerospace Systems." U.S. Military Specification MIL-B-5087B, October 15, 1964.

9.31 Plumer, J.A., and Robb, J.D.: "The Direct Effects of Lightning on Aircraft." IEEE Trans. on Electromag. Comp., EMC-24, 1982, pp. 158–172.

9.32 Society of Automotive Engineers: “Lightning Test Waveforms and Techniques for Aerospace Vehicles and Hardware.” Report of SAE Committee AE-4, Special Task F, May 5, 1976.

9.33 Society of Automotive Engineers: “Lightning Test Waveforms and Techniques for Aerospace Vehicles and Hardware.” Report of SAE Committee AE-4L, June 20, 1978.

9.34 U.S. Department of Defense: “Lightning Qualification Test Techniques for Aerospace Vehicles and Hardware.” U.S. Military Standard MIL-STD-1757, June 17, 1980.

9.35 U.S. Department of Defense: “Lightning Qualification Test Techniques for Aerospace Vehicles and Hardware.” U.S. Military Standard MIL-STD-1757A, 20 June 1983.

9.36 Federal Aviation Administration: “Protection of Airplane Fuel Systems Against Fuel Vapor Ignition Due to Lightning.” U.S. FAA Advisory Circular 20-53A, Washington, DC, April 12, 1985.

9.37 National Aeronautics and Space Administration: “Lightning Protection Criteria Document,” NSTS-07636, Lyndon B. Johnson Space Center, 1973.

9.38 Perala, R.A., Rudolph, T., and Eriksen, F.: “Electromagnetic Interaction of Lightning With Aircraft.” IEEE Trans. on Electromag. Comp., EMC-24, 1982, pp. 173–203.

9.39 U.S. Department of Defense: “Lightning Protection of Aerospace Vehicles and Hardware,” DOD Standard DOD-STD-1795, May 30, 1986.

9.40 Saint Privat d’Allier Research Group: “Eight Years of Lightning Experiments at Saint Privat d’Allier.” Revue Generale de l’Electricite, No. 9, 1982, pp. 561–582.

9.41 Hubert, P., Laroche, P., Eybert-Berard, A., and Barret, L.: “Triggered Lightning in New Mexico.” Journal of Geo. Research, vol. 89, 1984, pp. 2511–2521.

9.42 Leteinturier, C., Weidman, C., and Hamelin, J.: “Current and Electric Field Derivatives in Triggered Lightning Return Strokes.” Journal of Geo. Research, vol. 95, 1990, pp. 811–828.

9.43 Eybert-Berard, L., Barret, L., and Berlandis, J.P.: “Campagne Foudre aux Etats Unis, Kennedy Space Center (Florida), Programme RTLP 85.” Report SST/ASP 86-01. Centre d’Etudes Nucleaires de Grenoble, Box 85 X, 38041 Grenoble Cedex, France, 1986 (in French).

9.44 Barret, L., Boulay, G., and Eybert-Berard, A.: “Campagne Foudre RTLP 86, Kennedy Space Center (Florida) USA, Recueil des Resultats Bruts au 01.12.86.” Report STT/ASP 86-12/LB-mA. Centre d’Etudes Nucleaires de Grenoble, Box 85 X, 38041 Grenoble Cedex, France, 1986 (in French).

9.45 Eybert-Berard, A., Barret, L., and Berlandis, J.P.: “Campagne d’Experimentations Foudre RTLP 1987 (NASA Kennedy Space Center, Florida, USA).” Report STT/Lasp 88-21-AEB/LB/JPB-pD. Centre d’Etudes Nucleaires de Grenoble, Box 85 X, 38041 Grenoble Cedex, France, 1988 (in French).

9.46 Eybert-Berard , A., Barret, L., Berlandis, J.P., and Terrier, G.: "Characterisations des Decharges Electomagnetiques Provoquees, Campagne RTLP 1988, NASA Kennedy Space Center, Florida (USA)." Report STT/LASP 89-21/AEB/LB/JPB/GT-pD. Centre d'Etudes Nucleaires de Grenoble, Box 85 X, 38041 Grenoble Cedex, France, 1989 (in French).

9.47 Johnson, Dale L. and William W. Vaughan: "NASA Kennedy Space Center Peak Lightning Current Probabilities: Analysis and Assessment,", NASA TM-1999-TBD, 1999.